

The Multi-Band Magnification Bias for Gravitational Lenses

J. Stuart B. Wyithe¹, Joshua N. Winn², David Rusin

Harvard-Smithsonian Center for Astrophysics, 60 Garden St., Cambridge, MA 02138

swyithe@cfa.harvard.edu; jwinn@cfa.harvard.edu; drusin@cfa.harvard.edu

ABSTRACT

We present a generalization of the concept of magnification bias for gravitationally-lensed quasars, in which the quasars are selected by flux in more than one wavelength band. To illustrate the principle, we consider the case of two-band selection, in which the fluxes in the two bands are uncorrelated, perfectly correlated, or correlated with scatter. For uncorrelated fluxes, we show that the previously-held result—that the bias is the product of the single-band biases—is generally false. We demonstrate some important properties of the multi-band magnification bias using model luminosity functions inspired by observed correlations among X-ray, optical, infrared and radio fluxes of quasars. In particular, the bias need not be an increasing function of each flux, and the bias can be extremely large for non-linear correlations. The latter fact may account for the high lensing rates found in some X-ray/optical and infrared/radio selected samples.

Subject headings: Cosmology: gravitational lensing

1. Introduction

If a massive galaxy lies along the line of sight to a background quasar, the galaxy may act as a gravitational lens, magnifying and forming multiple images of the quasar. Beginning with the pioneering work of Turner, Ostriker, & Gott (1984), many authors have computed the number of lenses that should appear in well-defined samples of quasars, with particular attention given to the dependence of this statistic on the vacuum energy density (Turner 1990; Kochanek 1996; Helbig et al. 1999; Sarbu, Rusin, & Ma 2001; Li & Ostriker 2002).

¹Hubble Fellow

²NSF Astronomy & Astrophysics Postdoctoral Fellow

These calculations must take into account not only the probability that a massive galaxy will be aligned closely enough with a background quasar (the lensing cross-section), but also the enhancement of the quasar flux due to lensing (the magnification bias). This is because quasar samples are usually defined by observed flux in some wavelength band, and gravitational lensing boosts the observed flux, thereby sampling a fainter portion of the quasar luminosity function. For example, if intrinsically faint quasars are sufficiently more numerous than bright quasars, then a quasar with a given observed flux is more likely to be lensed than the cross-section alone would imply.

More recently attention has turned toward the information about galaxy mass profiles that can be gleaned from lens statistics. These statistics include lensing rates (see, e.g., Keeton & Madau 2001; Wyithe, Turner, & Spergel 2001; Li & Ostriker 2002), the ratio of four-image to two-image lenses (see, e.g., Rusin & Tegmark 2001; Finch et al. 2002), the image separation distribution (see, e.g., Kochanek & White 2001) and the brightness distribution of central images (see, e.g., Rusin & Ma 2001; Keeton 2001, 2002; Evans & Hunter 2002; Oguri 2002). All of these applications of lens statistics require a good understanding of magnification bias.

Borgeest, von Linde, & Refsdal (1991) noted that quasar samples selected by both radio and optical flux measurements are subject to what they called a “double magnification bias.” If the radio and optical fluxes from a given quasar are nearly independent, then quasars bright in both bands are especially likely to be lensed³. By assuming that gravitational lensing produces only one possible value of magnification, and using power-law luminosity functions for the optical and radio bands, Borgeest, von Linde, & Refsdal (1991) showed that the resulting two-band magnification bias is the product of the bias factors computed separately for each band.

It is timely to revisit the issue of multi-band magnification bias with a more general approach. With the advent of large-area sky surveys at many wavelengths, it has become possible to define samples of thousands of quasars by their observed fluxes in X-ray, optical, infrared, and radio bands. Quasars appear in large numbers in, for example, the RASS (ROSAT All-Sky Survey: Truemper 1982; Voges et al. 1999) and eventually ChaMP (Chandra Multi-wavelength Project: Wilkes et al. 2001; Silverman et al. 2002) at X-ray wavelengths; NVSS (NRAO-VLA Sky Survey: Condon et al. 1998) and FIRST (Faint Images of the Radio Sky at Twenty centimeters: Becker, White, & Helfand 1995; White et al. 1997) at radio

³Note that the important property of the two bands is independence, not a large separation in wavelength (as has since been stated in the literature; Bade et al. (1997)), although of course these two properties are related.

wavelengths; 2MASS (Two Micron All Sky Survey: Kleinmann et al. 1994) at near-infrared wavelengths; and SDSS (Sloan Digital Sky Survey: York et al. 2000; Schneider et al. 2002) at optical wavelengths. Cross-correlation of these catalogs (see, e.g., McMahon et al. 2001; Ivezić et al. 2002) will become an increasingly important source of information about quasars in general, and gravitational lens statistics in particular.

A few lenses have already been discovered using multi-band selection criteria, at lensing rates that are larger than the 0.2–1% typical of single-band lens surveys. Bade et al. (1997) discovered the gravitational lens RX J0911.4+0551 by matching RASS sources with optical sources from Schmidt plates. Of the ~ 40 radio-quiet X-ray-luminous high-redshift quasars known, two are lensed (Wu, Bade, & Beckmann 1999). A search for very red quasars through the matching of FIRST and 2MASS has identified two gravitational lenses out of thirteen sources (Gregg et al. 2002; Lacy et al. 2002). None of these projects were designed explicitly to discover gravitational lenses, although this is a realistic possibility for the future.

In this paper we investigate the magnification bias for quasar samples defined by measurements in multiple wavelength bands. After presenting the basic formalism for N bands (§2), we specialize to the case of two bands and consider some illustrative examples. We consider the cases in which the two fluxes are uncorrelated (§2.1), perfectly correlated (§2.2), and correlated with non-zero scatter (§2.3). We then use a realistic model of the optical luminosity function for quasars to demonstrate a few interesting properties of the multi-band magnification bias (§3); in particular, the bias does not necessarily increase with flux in each band, and there is a profound difference between the case of a linear correlation and a non-linear correlation with flux in another band. Finally, in §4 we summarize our results, and discuss possible applications of this formalism to real quasar samples.

2. Magnification Bias and the Multiple Imaging Rate

We begin by reviewing the case of single-band magnification bias (Turner 1980; Turner, Ostriker, & Gott 1984). In a sample of quasars at redshift z with (apparent⁴) luminosity L_1 , the fraction of multiple-image lensed quasars is

$$F(L_1, z) \approx \frac{B_1 \tau_{\text{mult}}}{B_1 \tau_{\text{mult}} + (1 - \tau_{\text{mult}})}, \quad (1)$$

where τ_{mult} is the cross-section for multiple imaging, and $B_1(L_1)$ is the magnification bias. For $\tau_{\text{mult}} \ll 1$ and $B_1 \tau_{\text{mult}} \ll 1$, this reduces to the usual expression $F(L_1, z) = B_1 \tau_{\text{mult}}$. The

⁴By “apparent,” we mean that L_1 is the luminosity inferred from the observed flux and the luminosity distance, without taking into account the possible magnification due to lensing.

magnification bias is evaluated as

$$B_1(L_1, z) = \frac{\int_0^\infty \frac{d\mu}{\mu} \frac{dP}{d\mu} \Phi_1(L_1/\mu, z)}{\Phi_1(L_1, z)}, \quad (2)$$

where $\Phi_1(L_1, z)$ is the quasar luminosity function, μ is the sum of the unsigned magnifications of the multiple images, and $\frac{dP}{d\mu}$ is the probability distribution for μ , taken for a singular isothermal sphere throughout the paper ($dP = 8\mu^{-3}d\mu$ for $\mu \geq 2$). This expression can be understood as a likelihood ratio. The denominator is the likelihood that the quasar is drawn from the sample of unlensed quasars with luminosity L_1 (within dL_1). The numerator is the likelihood that the quasar is drawn from the fainter sample of quasars with luminosity L_1/μ (within dL_1/μ), summed over all possible values of μ .

Understood this way, the generalization to N bands is straightforward. We require knowledge of the multivariate luminosity function, $\Phi_N(L_1, L_2, L_3, \dots, L_N, z)$. For a point source, the magnification is the same for all bands, because gravitational lensing is achronatic⁵. The multi-band magnification bias is therefore

$$B_{1\dots N}(L_1, L_2, L_3, \dots, L_N, z) = \frac{\int_0^\infty d\mu \frac{1}{\mu^N} \frac{dP}{d\mu} \Phi_{1\dots N}(L_1/\mu, L_2/\mu, L_3/\mu, \dots, L_N/\mu, z)}{\Phi_{1\dots N}(L_1, L_2, L_3, \dots, L_N, z)}. \quad (3)$$

The dependence of B on the apparent luminosities of the quasars depends on the correlations, if any, between the intrinsic luminosities of the quasars in those bands. To illustrate the interesting properties that can result, in the following sections we concentrate on the simplest non-trivial case, the two-band magnification bias. All of the results are easily generalized to N bands.

2.1. Two-Band Magnification Bias: No Correlation

Borgeest, von Linde, & Refsdal (1991) considered quasars observed at both optical and radio wavelengths, and assumed a power-law luminosity function for each band. They

⁵Gravitational lensing magnification is sensitive to source size. Therefore if the emission regions for the two bands differ greatly in their spatial extent, then there is the possibility of wavelength-dependent magnification. For example, the small optical emission region of a quasar may be microlensed by stars in the lensing galaxy, whereas the more extended emission regions at infrared or radio wavelengths is not generally microlensed (see Wyithe & Turner (2002) for a recent discussion of microlensing and magnification bias). We ignore the possibility of microlensing in this paper, but note that since the mean magnification of microlensed sources equals the magnification of un-microlensed sources, the results presented will be qualitatively correct, even for correlations involving bands that are subject to microlensing.

showed that if the fluxes in these bands are statistically independent, and if there is only one possible value of the lensing magnification, then the two-band magnification bias is equal to the product of the biases that would be computed separately for the optical and radio bands. This result is not true in general. As we show below, even if the two bands are independent, the result does not hold because real gravitational lenses produce a distribution of magnifications.

First, we reproduce the result of Borgeest, von Linde, & Refsdal (1991) using our formalism. For $N = 2$, Eq. (3) is

$$B_{12}(L_1, L_2, z) = \frac{\int_0^\infty \frac{d\mu}{\mu^2} \frac{dP}{d\mu} \Phi_{12}(L_1/\mu, L_2/\mu, z)}{\Phi_{12}(L_1, L_2, z)}. \quad (4)$$

If the bands are independent, then $\Phi_{12}(L_1, L_2, z) = \Phi_1(L_1, z)\Phi_2(L_2, z)$. The lens model used by Borgeest, von Linde, & Refsdal (1991) can be described by $\frac{dP}{d\mu} = \delta(\mu - \mu_0)$, in which case

$$B_{12}(L_1, L_2, z) = \frac{1}{\mu_0^2} \frac{\Phi_{12}(L_1/\mu_0, L_2/\mu_0, z)}{\Phi_{12}(L_1, L_2, z)} = \frac{1}{\mu_0^2} \frac{\Phi_1(L_1/\mu_0, z)\Phi_2(L_2/\mu_0, z)}{\Phi_1(L_1, z)\Phi_2(L_2, z)} = B_1(L_1, z)B_2(L_2, z). \quad (5)$$

This results fails for the more realistic case in which there is a range of possible magnifications, because $\frac{dP}{d\mu}$ appears once in the numerator of the multi-band magnification bias, but appears separately in each numerator in the product of the single-band biases. For example, following Borgeest, von Linde, & Refsdal (1991), suppose $\Phi_1(L_1, z) = \Phi_{1,*}L_1^{\alpha_1}$ and $\Phi_2(L_2, z) = \Phi_{2,*}L_2^{\alpha_2}$. If we adopt the magnification distribution appropriate for an isothermal sphere ($\frac{dP}{d\mu} = \frac{8}{\mu^3}$ for all $\mu \geq 2$), then

$$B_{12}(L_1, L_2, z) = \int_2^\infty \frac{d\mu}{\mu^2} \frac{8}{\mu^3} \frac{1}{\mu^{\alpha_1} \mu^{\alpha_2}} = \frac{8}{4 + \alpha_1 + \alpha_2} 2^{-(4+\alpha_1+\alpha_2)}, \quad (6)$$

for $\alpha_1 + \alpha_2 > -4$. Analogous calculations of the single-band bias factors give

$$B_1(L_1, z)B_2(L_2, z) = \frac{16}{(3 + \alpha_1)(3 + \alpha_2)} 2^{-(4+\alpha_1+\alpha_2)}, \quad (7)$$

which can be either larger or smaller than Eq. (6).

2.2. Two-Band Magnification Bias: Perfect Correlation

If the two bands are perfectly correlated, with $L_2 = f(L_1)$, one might expect that no new information is provided by the observation in the second band, and therefore that

the two-band bias is equal to the single-band bias for either band. This is not quite true. Gravitational magnification multiplies both fluxes by the same factor. If the unmagnified fluxes are linearly correlated, then the magnified fluxes also obey the correlation. However, if the correlation is non-linear, then the magnified fluxes do not obey the correlation, and the source must be gravitationally lensed. In the the appendix, we derive this result formally, by calculating the magnification bias for general correlations (see the next section) in the limit of zero scatter.

2.3. Two-Band Magnification Bias: Imperfect Correlation

More generally, L_1 and L_2 are correlated with some intrinsic scatter. On physical grounds we expect the magnitude of the scatter to scale with the luminosity [i.e. $\Delta L_2/L_2 \sim g(\Delta L_1/L_1)$], which makes it convenient to use logarithmic variables $l = \log L$. Suppose that the correlation between L_1 and L_2 is a power-law, $L_1 = L_2^\gamma$, or $l_1 = \gamma l_2$. Because of the correlation, it is convenient to express the luminosity function in terms of the new variables $u_1 \equiv \frac{1}{\gamma}l_1 + l_2$ and $u_2 \equiv -\gamma l_1 + l_2$, which describe the location parallel and perpendicular to the correlation, respectively (see Fig. 1). In these variables, the luminosity function (expressed in density per square logarithmic interval) is $\Psi_{12}(u_1, u_2, z) = (\gamma + \frac{1}{\gamma})\Phi_{12}(l_1, l_2, z)$. The luminosity function can also be written $\Psi_{12}(u_1, u_2, z) = \Psi_1(u_1, z)p(u_2|u_1, z)$, where $\Psi_1(u_1, z)$ is the luminosity function in the new variable u_1 and $p(u_2|u_1, z)$ is the conditional probability of u_2 given u_1 . Because we expect the scatter to be symmetric in reflection about the correlation⁶, we assume $p(u_2|u_1, z)$ to be Gaussian with variance σ , hence

$$\Psi_{12}(u_1, u_2, z) = \Psi_1(u_1, z) \frac{1}{\sqrt{2\pi}\sigma} \exp\left(-\frac{u_2^2}{2\sigma^2}\right). \quad (8)$$

Defining $M = \log \mu$, the magnification bias is

$$\begin{aligned} B_{12}(l_1, l_2, z) &= \int_0^\infty dM \frac{dP}{dM} \frac{\Phi_{12}(l_1 - M, l_2 - M, z)}{\Phi_{12}(l_1, l_2, z)} \\ &= \int_0^\infty dM \frac{dP}{dM} \frac{(\gamma + \frac{1}{\gamma})\Psi_{12}\left[u_1 - (1 + \frac{1}{\gamma})M, u_2 + (\gamma - 1)M, z\right]}{(\gamma + \frac{1}{\gamma})\Psi_{12}(u_1, u_2, z)}. \end{aligned} \quad (9)$$

⁶As an example of why we expect the scatter to be symmetric in reflection about the correlation, consider a sample of quasars with flux measured in two optical wave bands, say r and i . We would expect to find a variation of bias with i -band at fixed r -band that is qualitatively similar to the variation with r -band at fixed i -band. This symmetry in the magnification bias requires symmetry of the scatter in reflection about the correlation. We therefore choose to model the scatter as a symmetric function in logarithms of luminosity; that is, defined normal to the correlation (i.e. along the u_2 axis).

Inserting Eq. (8),

$$B_{12}(l_1, l_2, z) = \int_0^\infty dM' \frac{dP}{dM'} \frac{\Psi_1[u_1 - M', z]}{\Psi_1(u_1, z)} \exp\left(-\frac{1}{2\sigma^2} \left[\left(u_2 + \frac{\gamma(\gamma-1)}{1+\gamma} M' \right)^2 - u_2^2 \right]\right), \quad (10)$$

where we have defined $M' = (1 + \frac{1}{\gamma})M$. This expression illustrates many important points. First, if the correlation is linear ($\gamma = 1$) then B_{12} is independent of u_2 , and the contours of constant bias run normal to the correlation (i.e. along lines of constant $l_2 + l_1$). Furthermore, if $\Psi_1(u_1, z)$ is a monotonically decreasing function of u_1 , then we find that $B_{12}(l_1, l_2, z)$ is an increasing function of both l_1 and l_2 (since u_2 increases monotonically with both l_1 and l_2). This example will be further explored in Case 1 of §3. Eq. (10) also demonstrates the behavior arising from non-linear correlations ($\gamma \neq 1$). Here the exponential plays an important role; it introduces an asymmetry in the bias across the correlation. If, for example, $\gamma > 1$, then large biases can result from negative values of u_2 (i.e. below the correlation), because the exponent becomes positive. On the other hand, the exponent is negative for all $u_2 > 0$, and hence the bias above the correlation is small. This example will be further explored in Case 3 of §3.

In the following section, we evaluate Eq. 10 numerically, with more realistic assumptions, in order to illustrate these and other interesting and potentially observable properties of the multi-band magnification bias.

3. Magnification Bias for Illustrative Bi-Variate Luminosity Functions

We consider measurements made in two bands, and a power-law correlation between the two bands: $L_2 = L_1^\gamma$. As in §2.3, the scatter (normal to the correlation) is assumed to be Gaussian in logarithms with half-width σ . We consider 4 examples of Eq. (8). The first two examples involve linear correlations ($\gamma = 1$), and the second two examples involve non-linear correlations.

For the first of the two correlated bands, we use a luminosity function $\Phi_1(L_1, z)$ that is appropriate for optical wavelengths. A good representation of the observed optical quasar luminosity function at redshifts $z \lesssim 3$ is provided by the following double power-law form (Boyle, Shanks, & Peterson 1988; Pei 1995):

$$\Phi_o(L, z) = \frac{\Phi_*/L_*(z)}{[L/L_*(z)]^{\beta_l} + [L/L_*(z)]^{\beta_h}}. \quad (11)$$

At the faint end, the logarithmic slope of this function is $-\beta_l = -1.58$, while at the bright end the slope is $-\beta_h = -3.43$ (Boyle et al. 2000). Moreover, all dependence on redshift (for

$z \lesssim 3$) is in the break luminosity $L_*(z)$. We therefore show the luminosity function in units of L_* throughout the remainder of this paper. Setting $\Phi_1(L_1) = \Phi_o(L_1)$, we find from Eq. 8 that $\Phi_o(L_1)$ is related to $\Psi_1(u_1, u_2)$ through

$$\Phi_o(L_1) = \int_0^\infty dL_2 \Psi_1(u_1) \frac{1}{\sqrt{2\pi}\sigma} \exp\left(-\frac{u_2^2}{2\sigma^2}\right). \quad (12)$$

This equation defines the functions $\Psi_1(u_1)$ used in this section.

1. $\gamma = 1.0, \sigma = 0.15$: A linear correlation with constant scatter. This is the situation that might be expected between two different optical bands. The contours of Φ_{12} (gray), and of B_{12} (black), are shown in the top left panel of Fig. 2. As was derived in the previous section (and might be expected intuitively), the bias increases monotonically with both luminosities, and is constant along lines normal to the correlation.

The top right panel shows the corresponding single-band luminosity function (gray line), and magnification bias (dotted black line). These functions are the same for both bands because of the linear correlation. In addition we plot $B_{12}(L_1, L_2)$ for two paths through (L_1, L_2) -space: one at fixed L_1 (thick dashed line, plotted as a function of L_2) and the other below but parallel to the correlation (thin dashed line, plotted as a function of L_1).

2. $\gamma = 1.0, \sigma = 0.15 - 0.02 \log u_1$: Same as the previous example, except in this case we allow the logarithmic scatter to depend on luminosity. The results are shown in the lower panels of Fig. 2, in the same format as the previous example.

The contours of magnification bias wrap around the contours of Φ_{12} , increasing rapidly as one moves normal to the correlation (along the u_2 axis). This can be understood as follows. Magnification draws quasars from regions of lower intrinsic luminosity, where the probability density of quasars (as given by Φ_{12}) is larger. This is especially true when the observed luminosities fall at some distance from the correlation, because the scatter in the correlation is larger at lower luminosities.

The dependence of B_{12} on L_2 , for fixed L_1 , is again shown by the thick dark dashed line. Interestingly, the dependence is not monotonic. For small values of L_2 the magnification bias is large. The bias decreases as L_2 rises through the expected intrinsic value, and then increases again. The bias along the path denoted by the thin dashed line demonstrates that the bias can become very large for sources below the correlation.

3. $\gamma = 1.5, \sigma = 0.2$: A non-linear correlation with a constant scatter. This situation approximates the correlation that has been observed between the X-ray (L_2) and optical

(L_1) bands for quasars (Brinkmann et al. 2000). Results for this case are shown in the top two panels of Fig. 3, in the same format as the previous examples.

In this case, $\Phi_2(L_2)$ (thin gray line) is a flatter function than $\Phi_1(L_1)$ (thick gray line), and therefore the single-band bias B_2 (thin dotted line) is smaller than B_1 (thick dotted line). Although B_{12} is an increasing function of L_1 , it is actually a decreasing function of L_2 (for fixed L_1). This runs counter to the naive expectation that the brighter the quasar is (regardless of band), the more likely it is to be lensed. The reason is that when L_2 is smaller than expected from the correlation, reducing both luminosities by the same factor μ (along a line of unit slope, in the top left panel) brings one to a region of much higher probability.

4. $\gamma = -1.0$, $\sigma = 0.3$: An anti-correlation with constant scatter. This is a somewhat artificial example, but we might imagine there are two ways for a quasar with a fixed energy source to radiate its energy, and one of these ways can be blocked by a variable amount. For example, the optical and far-infrared luminosities might be expected to exhibit some degree of anti-correlation due to dust obscuration.

The results are plotted in the lower panels of Fig. 3. The contours of magnification bias are parallel to the anti-correlation. For small luminosities the bias is smaller than unity. Quasars in this region are *less* likely to be lensed than the cross-section alone would imply, because lensed quasars would be drawn from a population with very small density. Conversely, for large luminosities, the bias becomes arbitrarily large.

4. Discussion

The multi-band magnification bias is an *a posteriori* statistic. It is used to estimate the probability that the apparent luminosities of a given quasar, as measured in several bands, are due to gravitational magnification, rather than being intrinsic to the quasar. When a sample of quasars is selected through the matching of sources in two different catalogs, both fluxes must be used to perform this calculation. One must also have some knowledge of the intrinsic correlation (if any) of the fluxes, and the distribution of magnifications produced by lensing.

One might expect that the multi-band bias is maximized when the bands are uncorrelated (an example of which is shown for the radio-optical correlation of SDSS early data release quasars in Fig. 4), since in that case there is no redundant information in the flux measurements. Upon further reflection, or using the mathematics developed in this paper, one realizes that this is not true—the relevant information is how discrepant the observed

fluxes are from the correlation, and whether the discrepancy can be made smaller if the observed fluxes are all reduced by a constant factor.

Many of the illustrative examples presented in this paper approximate certain correlations that have been observed for real quasars. In particular, the multi-band magnification bias may result in very high lens fractions for certain quasar samples. First, we consider the case of a quasar sample selected by optical colors. The top left panel of Fig. 4 is a logarithmic plot of SDSS i -band *vs.* r -band fluxes for the SDSS early data release quasars (Schneider et al. 2002). The data show a linear correlation with scatter, the magnification bias for which is illustrated in the top panels of Fig. 2. The magnification bias must be computed using both optical measurements, unless the sample is 100% complete in one filter (i.e., unless after selecting quasars in i , the r -band magnitude was measured in every single case). As an example consider the sample of SDSS $z > 5.8$ quasars (Fan et al. 2001). Since the z -band selection is at $\sim 1100\text{\AA}$ in the rest-frame, quasars with fixed absolute B magnitude ($\sim 4400\text{\AA}$) are more likely to be selected if they are bluer than average. Thus a sample of quasars selected in this manner will be bluer than average and lie blueward of the correlation on a plot of the intrinsic correlation between M_V and M_B . The magnification bias for these sources may be significantly smaller than that computed using only extrapolations of the B -band luminosity function (Wyithe & Loeb 2002; Commerford, Haiman, & Schaye 2002).

Next, we consider examples of non-linear luminosity correlations. Brinkmann et al. (2000) measured the correlation between ROSAT X-ray and FIRST radio fluxes for matched quasar samples. They find that while radio-quiet quasars show a linear relationship between X-ray and radio luminosity, radio-loud quasars have an X-ray flux L_x that varies with the radio luminosity L_r as $L_x \propto L_r^{0.48 \pm 0.05}$ with an intrinsic scatter of ~ 0.2 dex. Furthermore, Brinkmann et al. (2000) showed that the X-ray luminosity correlates non-linearly with optical luminosity L_o , following $L_x \propto L_o^{1.42 \pm 0.09}$. The second of these correlations (in flux) is plotted in Fig. 4 for quasars in the SDSS Early Data Release (Schneider et al. 2002), but can be seen more clearly in Fig. 14 of Brinkmann et al. (2000). The multi-band magnification bias corresponding to the second correlation⁷ is illustrated in the top panels of Fig. 3. The magnification bias can be extremely large for sources that are luminous at both optical and X-ray wavelengths. This may be the explanation for the apparently high probability of lensing in bright X-ray selected quasar catalogs (Bade et al. 1997). The location of the gravitational lens RX J0911.4+0551, which was selected from cross-correlation of optical and X-ray catalogs, is shown on this plot by the large dot⁸. The fluxes place the quasar below

⁷Note that while we have presented results for a non-linear correlation with index $\gamma > 1$, the result for $\gamma < 1$ is simply obtained through reversal of the axes.

⁸We used the integrated R from Bade et al. (1997) and color transformations from Fukugita, Shimasaku

the correlation, in the region where we expect the magnification bias to be large (see the upper panels of Fig. 3). The lens HE 1104–1805 is also X-ray loud (Wisotzki et al. 1993; Reimers et al. 1995). While this lensed quasar was not discovered through cross-correlation between catalogs, it is interesting to note its location on this plot, shown by the open square in Fig. 4. The quasar is found to be very bright in both bands, and is again in the region of high magnification bias. It is suggestive that the two X-ray loud gravitational lenses both appear to lie in the region of high magnification bias, as expected.

Finally, the multi-band magnification bias may also provide an explanation for the large gravitational lens fraction (2 out of 13) found through the matching of FIRST and 2MASS sources (Gregg et al. 2002; Lacy et al. 2002). Fig. 4 shows the correlation for near infrared luminosities versus radio luminosities compiled from table 1 of Barkhouse & Hall (2001). The radio/near-IR correlation appears to be steeper than linear. If true we might expect very large biases for luminous near-IR sources. The top panel of Fig. 3 demonstrates magnification bias for a non-linear correlation, and shows that the bias of around 100 necessary to achieve a lens fraction of 2/13 is possible.

5. Summary

This paper has discussed the multi-band magnification bias for gravitational lensing with arbitrary luminosity functions in several bands. Previous discussion of the multi-band magnification bias (Borgeest, von Linde, & Refsdal 1991) focused on the case where the fluxes in the two bands are independent. If a single value for the lens magnification is considered, they showed that this assumption leads to a multiple magnification bias that is equal to the product of the single-band biases. However, we have shown that this equality breaks down in the more realistic case when there is a distribution of possible magnifications.

We also discussed the multi-band magnification bias when the fluxes in the various bands are correlated. In the case of a perfect (i.e. zero scatter) linear correlation, the information from the second band does not change the magnification bias. However, if the correlation is non-linear, then sources with fluxes that obey the correlation cannot be lensed. On the other hand, sources with fluxes that do not obey the correlation must be lensed.

Of course, real correlations have intrinsic scatter. We have calculated the multi-band magnification bias for bi-variate luminosity functions with finite scatter about both linear and non-linear correlations. For a linear correlation (as expected for a quasar sample selected

& Ichikawa (1995).

by optical colors) we find that the magnification bias is an increasing function of either flux. Calculations of lens statistics from incomplete color-selected quasar samples should therefore account for the multi-band magnification bias.

Non-linear correlations (and anti-correlations) with finite scatter were also explored. If the fluxes in two bands are correlated through a relation that is steeper than linear, then sources that lie below the correlation can be subject to a very large bias. The observed correlation between X-ray and optical flux (and possibly between infrared and radio flux) for quasars is steeper than linear. Suggestively, the two known X-ray loud gravitationally lensed quasars lie below the X-ray/optical correlation in the region of large magnification bias. Thus the multiple magnification bias may provide an explanation for the large lensing rates found in X-ray/optical and infrared/radio selected samples.

The authors wish to acknowledge discussions with Chris Kochanek that led us to work on this topic. We also thank Wai-Hong Tham and Lara Winn for enduring conversations. J.S.B.W. is supported by a Hubble Fellowship grant from the Space Telescope Science Institute, which is operated by the Association of Universities for Research in Astronomy, Inc., under NASA contract NAS 5-26555. J.N.W. is supported by an Astronomy & Astrophysics Postdoctoral Fellowship, under NSF grant AST-0104347.

REFERENCES

- Bade, N., Siebert, J., Lopez, S., Voges, W., & Reimers, D. 1997, *A&A*, 317, L13
- Barkhouse, W. A. & Hall, P. B. 2001, *AJ*, 121, 2843
- Becker, R. H., White, R. L., & Helfand, D. J. 1995, *ApJ*, 450, 559
- Borgeest, U., von Linde, J., & Refsdal, S. 1991, *A&A*, 251, L35
- Boyle, B.J., Shanks, T., & Peterson, B.A. 1988, *MNRAS*, 235, 935
- Boyle, B. J., Shanks, T., Croom, S. M., Smith, R. J., Miller, L., Loaring, N., & Heymans, C. 2000, *MNRAS*, 317, 1014
- Brinkmann, W., Laurent-Muehleisen, S. A., Voges, W., Siebert, J., Becker, R. H., Brotherton, M. S., White, R. L., & Gregg, M. D. 2000, *A&A*, 356, 445
- Commerford, J., Haiman, Z. & Schaye, J., 2002, *astro-ph/0206441*
- Condon, J.J., et al. 1998, *AJ*, 115, 1693

- Evans, N.W. & Hunter, C., 2002, astro-ph/0204206
- Fan, X. et al. 2001, AJ, 122, 2833
- Finch, T.K., Carlivati, L.P., Winn, J.N. & Schechter, P.L., 2002, astro-ph/0205489
- Fukugita, M., Shimasaku, K., & Ichikawa, T. 1995, PASP, 107, 945
- Gregg, M. D., Lacy, M., White, R. L., Glikman, E., Helfand, D., Becker, R. H., & Brotherton, M. S. 2002, ApJ, 564, 133
- Helbig, P., Marlow, D., Quast, R., Wilkinson, P. N., Browne, I. W. A., & Koopmans, L. V. E. 1999, A&AS, 136, 297
- Ivezic, Z., et al., 2002, astro-ph/0202408
- Keeton, C. R. 2001, ApJ, 561, 46
- Keeton, C. R. 2002, astro-ph/0206243
- Keeton, C. R. & Madau, P. 2001, ApJ, 549, L25
- Kleinmann, S. G. et al. 1994, Ap&SS, 217, 11
- Kochanek, C. S. 1996, ApJ, 466, 638
- Kochanek, C. S. & White, M. 2001, ApJ, 559, 531
- Koopmans, L.V.E. & Treu, T., 2002, ApJ, 568, L5
- Kundic, T., et al., 1997, ApJ, 482, 75
- Lacy, M., Gregg, M., Becker, R. H., White, R. L., Glikman, E., Helfand, D., & Winn, J. N. 2002, AJ, 123, 2925
- Li, L. & Ostriker, J. P. 2002, ApJ, 566, 65
- McMahon, R.G., Irwin, M.J., 1992, in Digitised Optical Sky Surveys, eds. H.T. MacGillivray & E.B. Thomson (Dordrecht: Kluwer), p417
- McMahon, R.G., White, R.L., Helfand, D.J. & Becker, R.H., 2001, astro-ph/0110437
- Oguri, M. 2002, astro-ph/0207520
- Pei, Y. C. 1995, ApJ, 438, 623

- Reimers, D., Bade, N., Scharstel, N., Hagen, H.-J., Engels, D., & Toussaint, F. 1995, *A&A*, 296, L49
- Rusin, D. & Ma, C.-P. 2001, *ApJ*, 549, L33
- Rusin, D. & Tegmark, M. 2001, *ApJ*, 553, 709
- Sarbu, N., Rusin, D., & Ma, C.-P. 2001, *ApJ*, 561, L147
- Schechter, P.L., et al. 1997, *ApJ*, 475, L85
- Schneider, D. P. et al. 2002, *AJ*, 123, 567
- Silverman, J.D., et al. 2002, *AJ*, 569, L1
- Truemper, J. 1982, *Advances in Space Research*, 2, 241
- Turner, E. L., Ostriker, J. P., & Gott, J. R. III 1984, *ApJ*, 284, 1
- Turner, E. L. 1990, *ApJ*, 365, L43
- Turner, E. L. 1980, *ApJ*, 242, L135
- Voges, W. et al. 1999, *A&A*, 349, 389
- Walsh, D., Carswell, R. F., & Weymann, R. J. 1979, *Nature*, 279, 381
- White, R. L., Becker, R. H., Helfand, D. J., & Gregg, M. D. 1997, *ApJ*, 475, 479
- Wilkes, B.J., et al. 2001, in *ASP Conf. Ser. 232, The New Era of Wide-Field Astronomy*, ed. R.G. Clowes, A.J. Adamson & G.E. Bromage (San Francisco: ASP), 47
- Wisotzki, L., Koehler, T., Kayser, R., & Reimers, D. 1993, *A&A*, 278, L15
- Wu, X., Bade, N., & Beckmann, V. 1999, *A&A*, 347, 63
- Wyithe, J. S. B., Turner, E. L., & Spergel, D. N. 2001, *ApJ*, 555, 504
- Wyithe, J. S. B., & Turner, E. L., 2002, *ApJ*, in press
- Wyithe, J. S. B., & Loeb, A. 2002, *ApJ*, in press
- York, D. et al., 2000, *AJ*, 120, 1579

A. Two-Band Magnification Bias for Perfect Correlations

In this appendix we derive the results mentioned in § 2.2 for the two-band magnification bias in the case of perfect correlations by taking the limit of small σ in Eq. (10). It is convenient to rewrite the exponential as follows

$$\lim_{\sigma \rightarrow 0} B_{12}(l_1, l_2, z) = \int_0^\infty dM' \frac{dP}{dM'} \frac{\Psi_1[u_1 - M', z]}{\Psi_1(u_1, z)} \lim_{\sigma \rightarrow 0} \exp \left(-\frac{1}{2\sigma^2} M' \frac{\gamma(\gamma-1)}{\gamma+1} \left[\frac{\gamma(\gamma-1)}{\gamma+1} M' + 2u_2 \right] \right). \quad (\text{A1})$$

First, consider the case of a linear correlation ($\gamma = 1$). In this case we find the exponential function is unity for all $\sigma > 0$, and Eq. (A1) reduces to

$$\lim_{\sigma \rightarrow 0} B_{12}(l_1, l_2, z) = \int_0^\infty dM' \frac{dP}{dM'} \frac{\Psi_1[u_1 - M', z]}{\Psi_1(u_1, z)} = \int_0^\infty dM \frac{dP}{dM} \frac{\Psi_1[2(l_1 - M), z]}{\Psi_1(2l_1, z)}. \quad (\text{A2})$$

Note that in this case we must have $l_1 = l_2$. We can relate $\Psi_1(u_1, z)$ to $\Phi_1(l_1, z)$ in the limit of small σ :

$$\begin{aligned} \lim_{\sigma \rightarrow 0} \Phi_1(l_1, z) &= \int_0^\infty dl_2 \lim_{\sigma \rightarrow 0} \Phi_{12}(l_1, l_2) = \int_0^\infty dl_2 \lim_{\sigma \rightarrow 0} \frac{\Psi_{12}(u_1, u_2)}{2} = \frac{1}{2} \int_0^\infty dl_2 \Psi_1(u_1) \delta(u_2) \\ &= \frac{1}{2} \int_0^\infty dl_2 \Psi_1(l_1 + l_2) \delta(l_1 + l_2) = \frac{1}{2} \Psi_1(2l_1). \end{aligned} \quad (\text{A3})$$

Thus, for a perfect linear correlation, we find that

$$\lim_{\sigma \rightarrow 0} B_{12}(l_1, l_2, z) = \int_0^\infty dM \frac{dP}{dM} \frac{\lim_{\sigma \rightarrow 0} \Phi_1[l_1 - M, z]}{\lim_{\sigma \rightarrow 0} \Phi_1(l_1, z)} = B_1(l_1, z), \quad (\text{A4})$$

which is the single band magnification bias. Therefore, if two luminosities obey a perfect linear correlation, the magnification bias is simply equal to the single-band magnification bias computed from either luminosity.

Next consider the case of a non-linear correlation ($\gamma \neq 1$). Specifically, we assume $\gamma > 1$ and $0 < M'_{\min} < M' < \infty$. Then

$$\begin{aligned} \lim_{\sigma \rightarrow 0} \exp \left(-\frac{1}{2\sigma^2} M' \frac{\gamma(\gamma-1)}{\gamma+1} \left[\frac{\gamma(\gamma-1)}{\gamma+1} M' + 2u_2 \right] \right) &= 0 && \text{if } u_2 > -\frac{\gamma(\gamma-1)}{\gamma+1} \frac{M'}{2} \\ &= 1 && \text{if } u_2 = -\frac{\gamma(\gamma-1)}{\gamma+1} \frac{M'}{2} \\ &= \infty && \text{if } u_2 < -\frac{\gamma(\gamma-1)}{\gamma+1} \frac{M'}{2} \end{aligned} \quad (\text{A5})$$

Note that only sources with $u_2 = 0$ or $u_2 < -\frac{\gamma(\gamma-1)}{\gamma+1} M'_{\min}$ are allowed. As a result we find that $\lim_{\sigma \rightarrow 0} B_{12}(l_1, l_2, z) = \infty$ if $u_2 < -\frac{\gamma(\gamma-1)}{\gamma+1} M'_{\min}$. Sources that lie on the correlation have

$u_2 = 0$, and therefore $\lim_{\sigma \rightarrow 0} B_{12}(l_1, l_2, z) = 0$. Thus if the correlation is non-linear, sources that lie on the correlation cannot be lensed, while sources that lie off the correlation must be lensed.

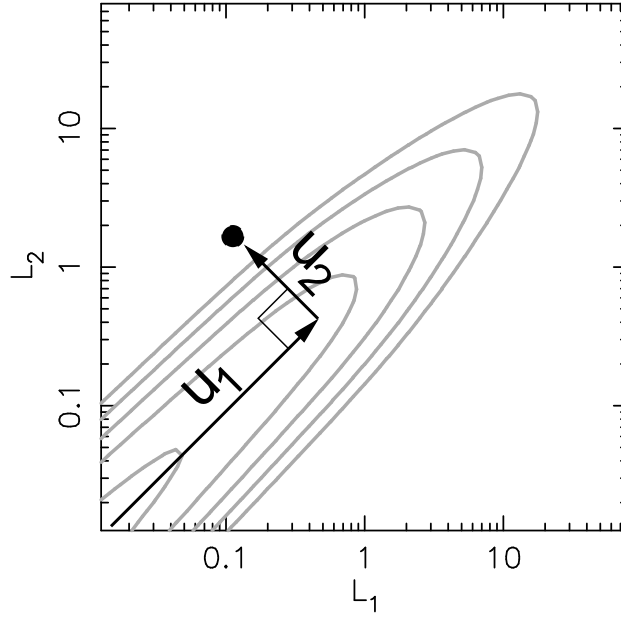


Fig. 1.— Schematic of variables defining the luminosity function for non-zero scatter about a power-law correlation. The grey lines are contours of a bi-variate luminosity function and are shown for context.

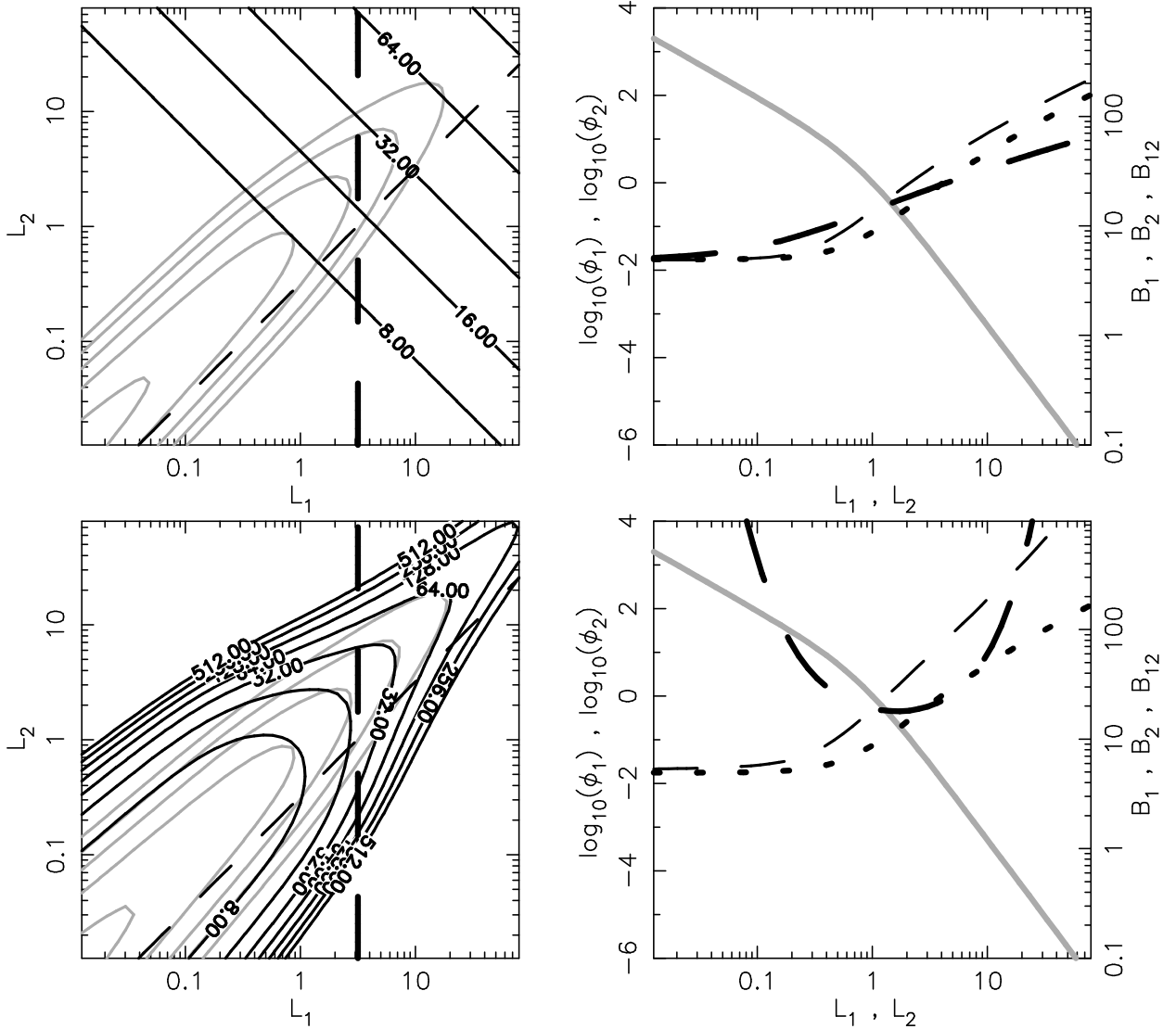


Fig. 2.— Bi-variate magnification biases for linear correlations with scatter. Top: Linear correlation, with a scatter that is insensitive to luminosity ($\gamma = 1.0$, $\sigma = 0.15$). Bottom: Linear correlation with a scatter that decreases with luminosity ($\gamma = 1.0$, $\sigma = 0.15 - 0.02 \log u_1$). The left hand panels show contours of the bi-variate luminosity function (grey lines). The solid lines are contours of magnification bias. The right hand panels show the corresponding single band luminosity functions (grey lines). Also shown are the single band magnification biases (dotted lines), and the magnification bias along the paths denoted by the dashed lines in the left hand figure. The bias for the path denoted by the thin dashed line is plotted as a function of L_1 , while the bias along the thick dashed line is plotted as a function of L_2 . Because of the linear correlation, the single band luminosity functions and magnification biases are identical for the two bands.

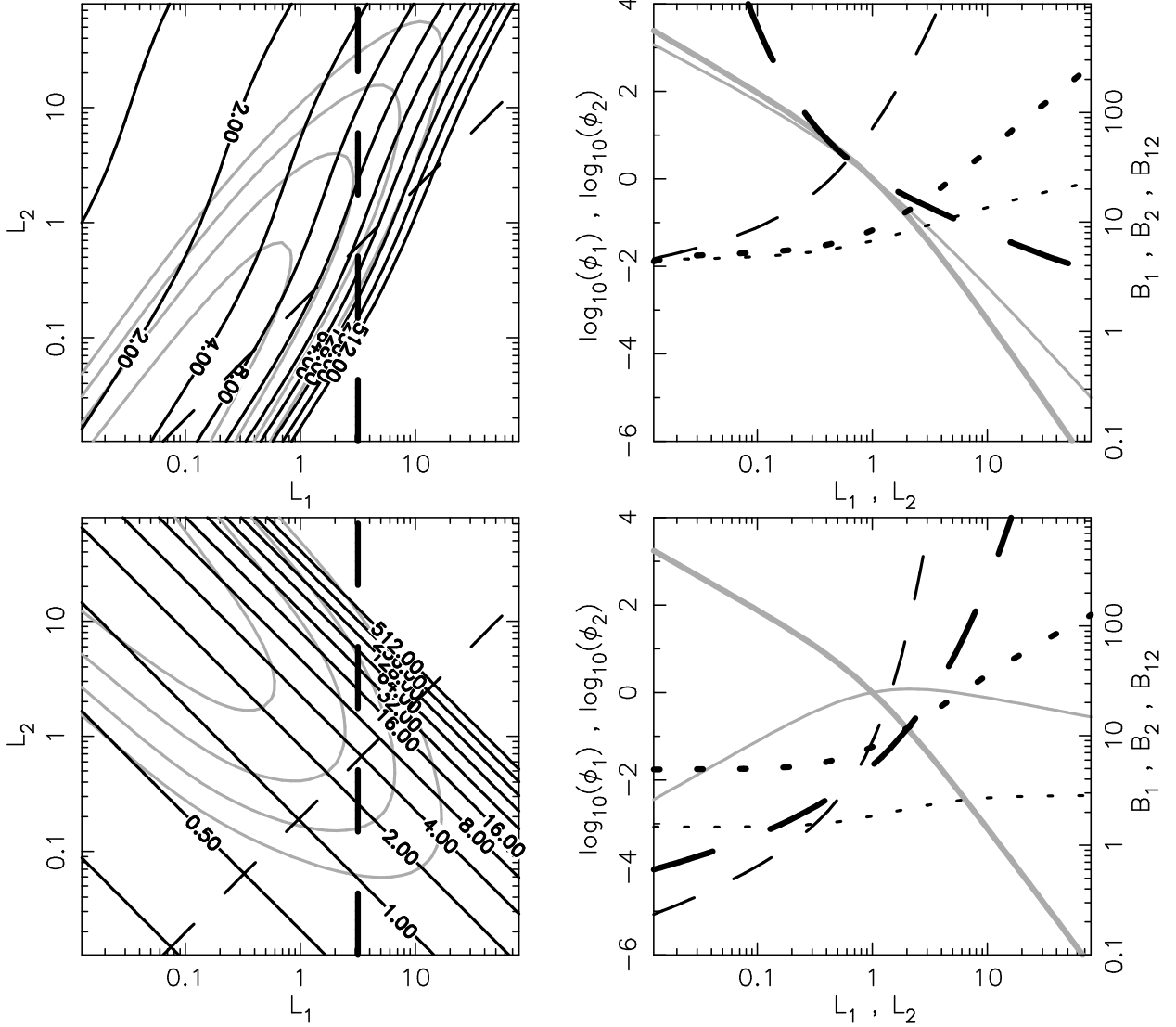


Fig. 3.— Bi-variate magnification biases for non-linear correlations with scatter. Top: Non-linear correlation, with a logarithmic scatter that is insensitive to luminosity ($\gamma = 1.5$, $\sigma = 0.2$). Bottom: Non-linear anti-correlation, with a logarithmic scatter that is insensitive to luminosity ($\gamma = -1.0$, $\sigma = 0.3$). The left hand panels show contours of the bi-variate luminosity function (grey lines). The solid lines are contours of magnification bias. The right hand panels show the corresponding single band luminosity functions (grey lines) and the single band magnification biases (dotted lines). Thick and thin lines denote quantities in L_1 and L_2 respectively. Also shown are the magnification biases along the paths denoted by the dashed lines in the left hand figure. The bias for the path denoted by the thin dashed line is plotted as a function of L_1 , while the bias along the thick dashed line is plotted as a function of L_2 .

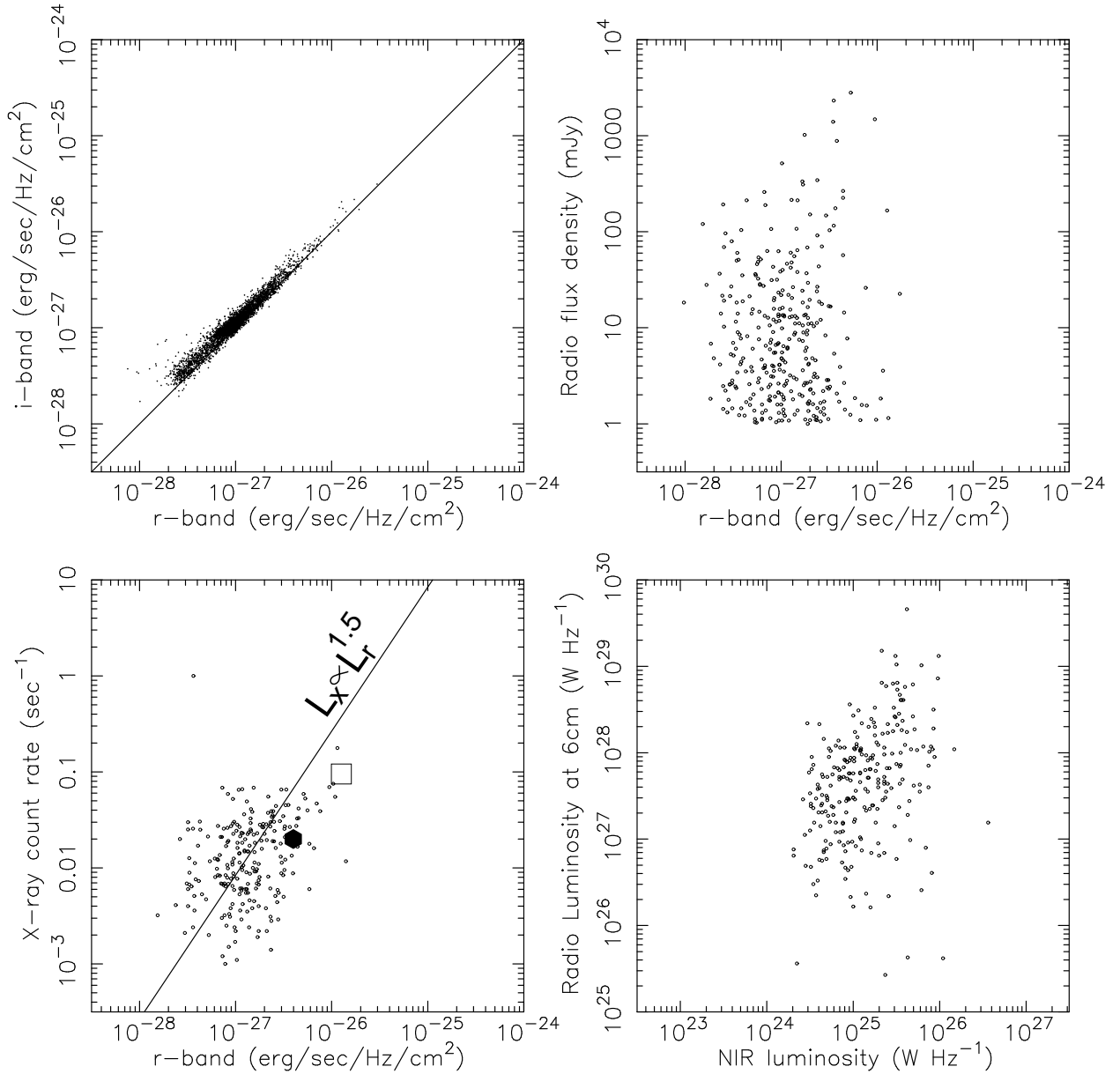


Fig. 4.— Correlations in different bands. Top Left: SDSS *i*-band vs. SDSS *r*-band flux. (Schneider et al. 2002) Top Right: FIRST radio flux vs. SDSS *r*-band flux (Schneider et al. 2002). Lower Left: ROSAT X-ray counts vs. SDSS *r*-band flux (Schneider et al. 2002) for quasars with redshifts larger than 0.5. The large dot in this panel represents RX J0911.4+0551, while the open square shows the location of HE 1104-1805. Bottom Right: Radio vs. Near IR luminosity (Barkhouse & Hall 2001). In the left hand panels the observed correlation lines are drawn to guide the eye.